



XXVth International Conference on Ultrarelativistic Nucleus-Nucleus Collisions
(Quark Matter 2017)

Measurements of charmonium production in p+p, p+Au, and Au+Au collisions at $\sqrt{s_{NN}} = 200$ GeV with the STAR experiment

Takahito Todoroki (for the STAR Collaboration)

Physics Department, Brookhaven National Laboratory, Upton, New York 11973, USA

Abstract

We present the first results from the STAR MTD of mid-rapidity charmonium measurements via the di-muon decay channel in p+p, p+Au, and Au+Au collisions at $\sqrt{s_{NN}} = 200$ GeV at RHIC. The inclusive J/ψ production cross section in p+p collisions can be described by the Non-Relativistic QCD (NRQCD) formalism coupled with the color glass condensate effective theory (CGC) at low transverse momentum (p_T) and next-to-leading order NRQCD at high p_T . The nuclear modification factor in p+Au collisions for inclusive J/ψ is below unity at low p_T and consistent with unity at high p_T , which can be described by calculations including both nuclear PDF and nuclear absorption effects. The double ratio of inclusive J/ψ and $\psi(2S)$ production rates for $0 < p_T < 10$ GeV/c at mid-rapidity between p+p and p+Au collisions is measured to be $1.37 \pm 0.42 \pm 0.19$. The nuclear modification factor in Au+Au collisions for inclusive J/ψ shows significant J/ψ suppression at high p_T in central collisions and can be qualitatively described by transport models including dissociation and regeneration contributions.

Keywords: heavy-ion collisions, quarkonium, J/ψ suppression, color screening, cold nuclear matter effect

1. Introduction

The J/ψ dissociation by the color-screening effect in the hot and dense medium [1] was initially proposed as direct evidence of the quark-gluon plasma formation. However, the interpretation of J/ψ suppression observed in heavy-ion collisions has remained a challenge due to the contribution of regenerated J/ψ from the coalescence of deconfined $c\bar{c}$ pairs in the medium as well as cold nuclear matter effects. Quantifying the cold and hot nuclear matter effects at the RHIC requires precise measurements of charmonium production in p+p, p+Au, and Au+Au collisions. The Muon Telescope Detector (MTD), which provides both the muon triggering and identification capabilities at mid-rapidity, opens the door to measuring quarkonia via the di-muon decay channel at STAR. Using the MTD di-muon trigger, the STAR experiment recorded data corresponding to an integrated luminosity of 14.2 nb^{-1} in Au+Au collisions at $\sqrt{s_{NN}} = 200$ GeV in the RHIC 2014 run, and integrated luminosities of 122 pb^{-1} in p+p collisions and 409 nb^{-1} in p+Au collisions at $\sqrt{s_{NN}} = 200$ GeV in the RHIC 2015 run. In these proceedings, we present (i) measurements of nuclear

modification factors for inclusive J/ψ production over a broad kinematic range in both p+Au and Au+Au collisions at $\sqrt{s_{NN}} = 200$ GeV; and (ii) the first measurement of the double ratio of inclusive $\psi(2S)$ and J/ψ production rates at mid-rapidity between p+p and p+Au collisions at $\sqrt{s_{NN}} = 200$ GeV.

2. Inclusive J/ψ measurements in p+p and p+Au collisions at $\sqrt{s_{NN}} = 200$ GeV

Figure 1 shows the production cross section of inclusive J/ψ in p+p collisions at $\sqrt{s} = 200$ GeV via the di-muon decay channel for the transverse momentum (p_T) range of $1 < p_T < 10$ GeV/c (red circles), along with a similar measurement via the di-electron decay channel in $0 < p_T < 14$ GeV/c. These results are consistent in the overlapping p_T range. The experimental results can be well described by CGC+NRQCD [2] and NLO NRQCD [3] calculations for prompt J/ψ at low and high p_T ranges, respectively. While an improved color evaporation model (ICEM) calculation for direct J/ψ [4] can describe the data for $p_T < 3$ GeV/c, it generally underestimates the yield at higher p_T .

Figure 2 shows the nuclear modification factor, R_{pAu} , of inclusive J/ψ in 0-100% central p+Au collisions. The measured R_{pAu} is generally consistent with the previous R_{dAu} result reported by the PHENIX experiment [5] within statistical and systematic uncertainties. The largest deviation between these results is 1.4σ in the range of $3 < p_T < 5$ GeV/c. This overall consistency suggests similar cold nuclear matter effects in p+Au and d+Au collisions. Calculations, taking into account the nuclear PDF effect using the nCTEQ15 [6, 7, 8] or EPS09NLO [6, 7, 8, 9] nuclear PDF sets, can touch the upper limit of the data within uncertainties. However, the model calculation including an additional nuclear absorption effect [10] is favored by the data.

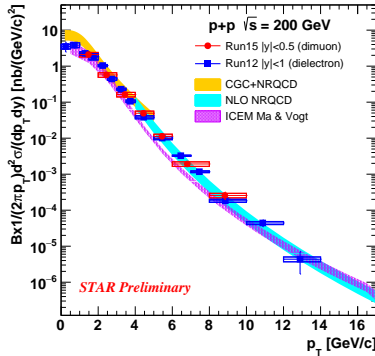


Fig. 1. Inclusive J/ψ production cross section scaled by the branching ratio (B) as a function of p_T in the di-muon (red circle) and the di-electron decay channels (blue square).

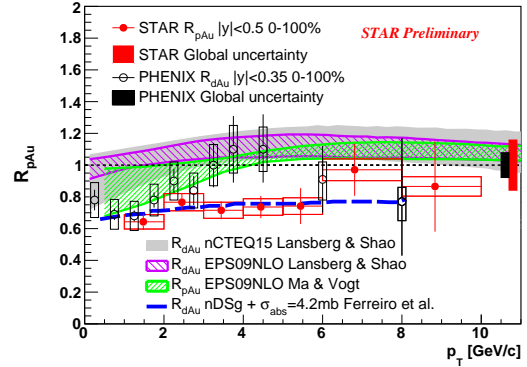


Fig. 2. Nuclear modification factor R_{pAu} as a function of p_T for inclusive J/ψ in the di-muon decay channel.

3. Double ratio of inclusive J/ψ and $\psi(2S)$ yields between p+p and p+Au collisions at $\sqrt{s_{NN}} = 200$ GeV

Figure 3 shows the ratio of inclusive J/ψ and $\psi(2S)$ production cross sections as a function of p_T in p+p collisions at $\sqrt{s} = 200$ GeV. The new STAR result for $0 < p_T < 10$ GeV/c follows the global trend of results by HERA [11], PHENIX [12, 13], and CDF [14] experiments. The ICEM calculation at $\sqrt{s} = 200$ GeV [4] can describe the increasing trend of the ratio with p_T .

Figure 4 shows the double ratio of $\psi(2S)$ and J/ψ production rates between p+p and p+Au collisions as a function of rapidity. The new STAR results at $|y| < 0.5$ is $1.37 \pm 0.42(\text{stat}) \pm 0.19(\text{sys})$, which is consistent with the published PHENIX results at $|y| < 0.35$ in d+Au collisions [15]. The co-mover model calculation [16, 17] can qualitatively describe the double ratio at forward and backward rapidities in p+Au collisions reported by the PHENIX experiment [13], and is consistent with the new STAR result at mid-rapidity within uncertainties.

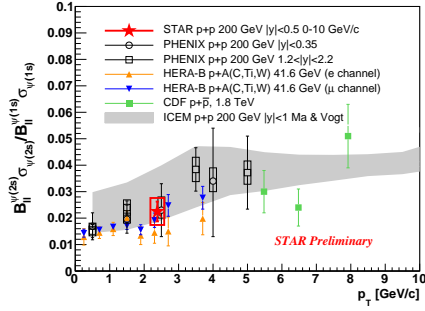


Fig. 3. Ratio of $\psi(2S)$ to J/ψ production rates as a function of p_T .

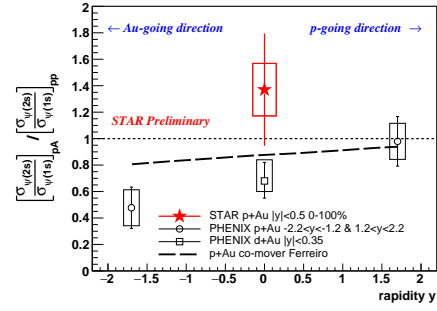


Fig. 4. Double ratio of J/ψ and $\psi(2S)$ production rates as a function of rapidity in p+Au and d+Au collisions.

4. Inclusive J/ψ measurements in Au+Au collisions at $\sqrt{s_{NN}} = 200$ GeV

Shown in Fig. 5 is the nuclear modification factor R_{AA} of inclusive J/ψ in 0-40% central Au+Au collisions compared with LHC results [18, 19]. The strong suppression at RHIC at high p_T indicates significant J/ψ dissociation. The hint of the increasing R_{AA} with increasing p_T can be explained by the formation-time effect and the feed-down contribution from B hadron decays [20]. The stronger suppression of J/ψ at RHIC at low p_T can be explained by less regeneration contribution due to smaller charm production cross section, while the smaller suppression of J/ψ at RHIC at high p_T could arise from a smaller dissociation rate due to the lower temperature of the medium. The R_{AA} as a function of the number of participant nucleons (N_{part}) for $p_T > 0$ GeV/c and $p_T > 5$ GeV/c are compared with the R_{pAu} in Fig. 6. The nuclear modification factors in the most peripheral Au+Au collisions are consistent with those measured in p+Au collisions.

Transport models from Tsinghua [21, 22] and Texas A&M University (TAMU) [20, 23] groups, including dissociation and regeneration contributions, can qualitatively describe the p_T dependence of the RHIC and the LHC data as shown in Fig. 5. Centrality dependences of the J/ψ R_{AA} at the RHIC [24] and the LHC are shown in Fig. 7 for $p_T > 0$ GeV/c and in Fig. 8 for $p_T > 5$ GeV/c. For $p_T > 0$ GeV/c, both models can describe the centrality dependence at the RHIC, but tend to overestimate the suppression at the LHC. For $p_T > 5$ GeV/c, there is tension among models and data. The discontinuities seen in the R_{AA} as a function of N_{part} from the Tsinghua model calculation can be attributed to the complete dissociation of J/ψ when the medium temperature exceeds the dissociation temperature.

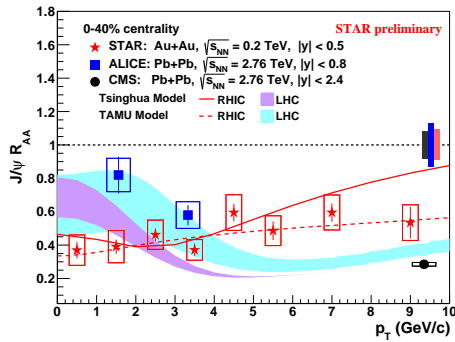


Fig. 5. R_{AA} as a function of p_T at the RHIC (red star) and the LHC (blue square, black circle). The lines and bands indicate transport model calculations for RHIC and LHC energies.

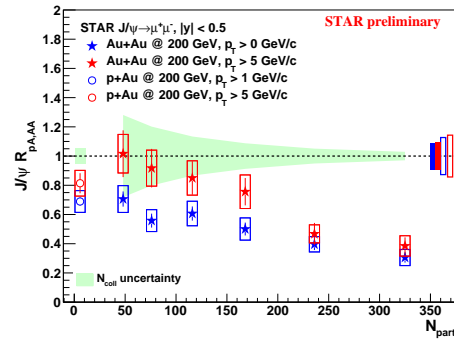


Fig. 6. R_{AA} (solid star) and R_{pAu} (open circle) for $p_T > 0(1)$ GeV/c and $p_T > 5$ GeV/c as a function of N_{part} .

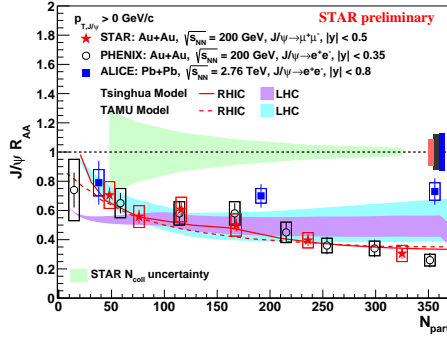


Fig. 7. Nuclear modification factor R_{AA} for $p_T > 0$ GeV/c as a function of N_{part} .

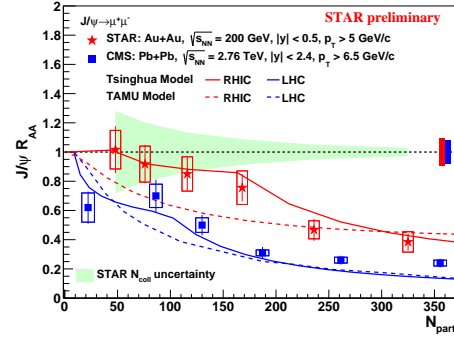


Fig. 8. Nuclear modification factor R_{AA} for $p_T > 5$ GeV/c as a function of N_{part} .

5. Summary

In summary, we presented the first charmonium measurements in the di-muon decay channel at mid-rapidity at the RHIC. In p+p collisions at $\sqrt{s} = 200$ GeV, inclusive J/ψ production cross section can be described by CGC+NRQCD and NLO NRQCD model calculations for prompt J/ψ at low and high p_T ranges, respectively. While the ICEM calculation for direct J/ψ can describe the data for $p_T < 3$ GeV/c, it generally underestimates the yield at higher p_T . In p+Au collisions at $\sqrt{s_{NN}} = 200$ GeV, we observe (i) inclusive J/ψ R_{pAu} is consistent with R_{dAu} suggesting similar cold nuclear matter effects in p+Au and d+Au collisions; (ii) calculations incorporating the nuclear PDF and nuclear absorption effects can well describe R_{pAu} ; and (iii) the double ratio of inclusive J/ψ and $\psi(2S)$ production rates between p+p and p+Au collisions is $1.37 \pm 0.42 \pm 0.19$. In Au+Au collisions at $\sqrt{s_{NN}} = 200$ GeV, we observe (i) significant J/ψ suppression in central collisions at high p_T indicating dissociation; (ii) the J/ψ R_{AA} can be qualitatively described by transport models including dissociation and regeneration; and (iii) the R_{AA} in the most peripheral collisions is consistent with the R_{pAu} . These measurements in Au+Au collisions will gain additional statistical precision by combining with the similar amount of data recorded in the RHIC 2016 run.

References

- [1] T. Matsui, H. Satz, Phys. Lett. B178 (1986) 416–422.
- [2] Y.-Q. Ma, R. Venugopalan, Phys. Rev. Lett. 113 (19) (2014) 192301.
- [3] H.-S. Shao, H. Han, Y.-Q. Ma, C. Meng, Y.-J. Zhang, K.-T. Chao, JHEP 05 (2015) 103.
- [4] Y.-Q. Ma, R. Vogt, Phys. Rev. D94 (11) (2016) 114029.
- [5] A. Adare, et al., Phys. Rev. C87 (3) (2013) 034904.
- [6] J.-P. Lansberg, H.-S. Shao, Eur. Phys. J. C77 (1) (2017) 1.
- [7] H.-S. Shao, Comput. Phys. Commun. 184 (2013) 2562–2570.
- [8] H.-S. Shao, Comput. Phys. Commun. 198 (2016) 238–259.
- [9] H.-S. Shao, R. Vogt, Private Communication (2017).
- [10] E. G. Ferreira, F. Fleuret, J. P. Lansberg, N. Matagne, A. Rakotozafindrabe, Few Body Syst. 53 (2012) 27–36.
- [11] I. Abt, et al., Eur. Phys. J. C49 (2007) 545–558.
- [12] A. Adare, et al., Phys. Rev. D85 (2012) 092004.
- [13] A. Adare, et al., Phys. Rev. C95 (3) (2017) 034904.
- [14] F. Abe, et al., Phys. Rev. Lett. 79 (1997) 572–577.
- [15] A. Adare, et al., Phys. Rev. Lett. 111 (20) (2013) 202301.
- [16] E. G. Ferreira, Private Communication (2016).
- [17] E. G. Ferreira, Phys. Lett. B749 (2015) 98–103.
- [18] B. B. Abelev, et al., Phys. Lett. B734 (2014) 314–327.
- [19] S. Chatrchyan, et al., JHEP 05 (2012) 063.
- [20] X. Zhao, R. Rapp, Phys. Rev. C82 (2010) 064905.
- [21] Y.-p. Liu, Z. Qu, N. Xu, P.-f. Zhuang, Phys. Lett. B678 (2009) 72–76.
- [22] K. Zhou, N. Xu, Z. Xu, P. Zhuang, Phys. Rev. C89 (5) (2014) 054911.
- [23] X. Zhao, R. Rapp, Nucl. Phys. A859 (2011) 114–125.
- [24] A. Adare, et al., Phys. Rev. Lett. 98 (2007) 232301.